Macromolecular Research

Article

DOI 10.1007/s13233-022-0070-4

www.springer.com/13233 pISSN 1598-5032 eISSN 2092-7673

Characterization of Opto-Electrical, Electrochemical and Mechanical Behaviors of Flexible PVA/(PANI+La_2CuO_4)/$LiClO_4$-PC Polymer Blend Electrolyte Films

Murad Q. A. Al-Gunaid*[,1]
Shashikala B. S.[2]
Gayitri H. M.[3]
Khaled Alkanad[4]
Nabil Al-Zaqri[5]
Ahmed Boshaala[6]
Fares H. Al-Ostoot*[,7,8]

[1] Department of Chemistry, Faculty of Education, Thamar University, Dhamar, Yemen
[2] Department of Physics, Sri Jayachamarajendra College of Engineering, JSS Science and Technology University, Mysore, India& Research Foundation, JSSTI Campus, Mysuru - 570 006, India
[3] Department of Electronics and Communication Engineering, JSS Science and Technology University, Sri Jayachamarajendra College of Engineering, Mysore 570006, India
[4] Department of Physics, University of Mysore, Mysore, India
[5] Department of Chemistry, College of Science, King Saud University, P.O. Box 2455, Riyadh, 11451, Saudi Arabia
[6] Research Centre, Manchester Salt & Catalysis, unit C, 88-90 Chorlton Rd, M15 4AN Manchester, United Kingdom
[7] Department of Biochemistry, Faculty of Education and Science, Albaydha University, Albaydha, Yemen
[8] Department of Biochemistry, University of Mysore, Mysuru, India

Received December 29, 2021 / Revised March 31, 2022 / Accepted April 19, 2022

Abstract: A new series of flexible nanocomposite-solid polymer electrolyte (SPEs) in the form of poly(vinyl alcohol) (PVA) impregnated by core-shells polyaniline (PANI)-La_2CuO_4 (20:2 wt%) of nanofillers, 10 wt% $LiClO_4$ as electrolyte and various amount 2, 4, 6, and 8 wt% of propylene carbonate, PC as plasticizer *via* solvent intercalation method. The obtained plasticized PVA-SPEs films were evaluated for their microstructural and morphological behaviors *via* X-ray diffraction (XRD), scanning electron microscopy (SEM), and Fourier transform infrared (FTIR) spectroscopy, respectively. The surface morphology of plasticized PVA-SPEs films illustrated the finer dispersion of inclusion fillers in the PVA matrix with increasing the dosage of PC content. FTIR spectra showed a reduction in the characteristic peaks of PVA in composite films and that denoted the interaction between PVA-OH and fillers. Optical findings exhibited higher absorbance of PVA-SPE in the visible region compared with pure PVA; in addition, the band-gap energy was reduced to 2.68 eV for PVA-SPE containing 8 wt% PC. The current-voltage characteristics showed a slight deviation for all PVA-SPE films denoting to non-ohmic behavior. Besides, the maximum ac-conductivity was found at 40.3×10^{-5} S/cm for PVA-SPE film containing 8 wt% PC with enhanced their specific capacitance by two folds compared with pure PVA. Mechanical testing showed that elongation at break has been increased attributed to increasing flexibility of polymeric segments with the increase in PC content.

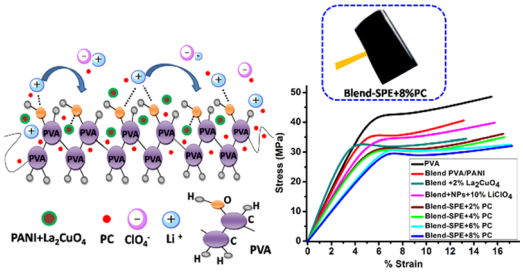

Keywords: PVA-SPEs, core-shell NCs, E_g, ac-conductivity, specific capacitance.

1. Introduction

The polymer electrolyte must have an advantage as flexibility, mouldability of shape and high electric properties for application purposes. There are several approaches were adopted to enhance the ionic-conductivity of SPEs to sensible levels and appropriate for applications. That approaches comprise the addition of plasticizers, utilize copolymers, and incorporation of nanofillers, usage of salts with large anions and blending of two polymers.[1-3] The polymeric blend is one of the most feasible approaches which offer a comfortable process, uncomplicated control during preparation and modifying physical characteristics within a compositional system. Solid polymer blends electrolyte (SPE) systems obtained by incorporating electrolyte salt into the mixture of different polymers in order to reduce the crystalline phase of the matrix in composites. These could improve the flexible and amorphous content required for faster ion transport, thus exhibiting higher ionic conductivity.[4,5] Conducting polymers are an organic polymer that has good electrical conductivity and can be used in various applications.[6-8] Through several conductive polymeric substances, polyaniline (PANI) is most useful for super-capacitors where it has suitable redox reversibility with high electric conduction, good environmental, chemical-electrical stability, and easy synthesis.[9-11] However, the low solubility, disability to forming film and very poor mechanical properties limit the applications of PANI. Currently, polyvi-

Acknowledgment: The authors are thankful to late. Dr. Siddaramaiah, Prof and Head, the department of Polymer Science and Technology, JSS Science and Technology University, Mysuru, India, for the support and guidance throughout this work. The authors extend their appreciation to the Researchers Supporting Project number (RSP-2021/396), King Saud University, Riyadh, Saudi Arabia.

***Corresponding Authors:** Fares H. Al-Ostoot (faresalostoot@gmail.com), Murad Q. A. Al-Gunaid (morad.jounid11@gmail.com)

nyl alcohol (PVA) is frequently employed in many applications, since its transparency to visible light, flexibility, excellent film formability with good mechanical properties and chemical stability; it is also low-cost and has hydrophilic nature. However, PVA has a low refractive index and poor electric property. Several literatures reported the performance of PVA can be enhanced with the inclusion of different fillers.[12,13]

Therefore, PANI was chosen as a secondary polymer for making a polymer blend along with PVA for the present polymer electrolyte to overcome the drawbacks, which exist in pure polymers. The strategy of the current investigation depends firstly on the core-shell particle composites process where the NPs encapsulated in the conducting PANI followed by blending them into the PVA matrix. The NPs encapsulated with conducting PANI was predominantly including chemical oxidative and electrochemical techniques.[14] The encapsulation is generally done ex-situ where the inorganic NPs are prepared separately and then added to the PANI matrix in certain compositions during the polymerization reaction.[15,16] The incorporation of the active nanomaterials into the host polymer is a promising approach to the synthesis of multi-functional nanocomposites (NCs), which can be used as catalysis, sensors, electrochromic display, electrodes for fuel cells, capacitors, *etc.*[17,18] Among an extensive variety of nanostructures, the perovskite lanthanum cuprate (La_2CuO_4 NPs) have received great attention for their applications including ferroelectrics, photo-electrics, catalysis and especially their superconductivity features at low temperatures.[19-21] The catalytic activity of La_2CuO_4 widens its potential uses in various redox reactions a substantial possibility of using it as electrode material. For further improvement of ionic conductivity of blend matrix based on PVA/(PANI+NPs); lithium salt and plasticizer are added in order to increase the amorphous portions with the inclusion of conducting ions in a polymeric blend. Enhancement in ionic-conductivity of plasticized-SPEs may be ascribed to the dissolution process of salt along with ionic effectiveness and reducing crystalline portions in polymeric composites.[22] The electric conduction of such blend-SPEs may attribute to molecular motions and movements of ions. Researchers are still working on a strategy for achieving high electrical conductivity, with desirable thermal and mechanical properties in a polymer structure, extremely necessary in a variety of uses like opto-electrical devices, electromagnetic shielding, and increased electric energy storage capacity.[23,24] In general, one of the most successful and cost-efficient ways to enhance electrical devices is to incorporate highly electrically conductive fillers into the polymer structure. There are several studies, which show an increase in conductivity of PVA after embedding with different filters.[25,26] Further, insufficient literature is available on the optical and conductivity of nanocomposite-solid polymer electrolyte in the form of flexible PVA/(PANI+La_2CuO_4)/$LiClO_4$ SPEs. Therefore, in this investigation, an endeavor was made to fabricate a new series of flexible films based on PVA/(PANI coated 2 wt% La_2CuO_4 NPs) complexed with 10 wt% $LiClO_4$ and varying amounts of plasticizer propylene carbonate, PC in order to achieve good conductivity at room temperature, reduction in optical bandwidth, increase refractive indices and mechanical features of PVA-SPE films.

2. Experimental

2.1. Materials

PVA (average m.wt 125,000 Aldrich), lithium perchlorate trihydrate [($LiClO_4.3H_2O$); analytical reagent (AR) grade], aniline, ammonium persulfate $(NH_4)_2S_2O8$ (APS), lanthanum (III) nitrate tri hydrate ($La(NO_3)_3.3H_2O$) as oxidants), and glycine ($C_2H_5NO_2$; as fuel) were purchased from S. D. Fine Chemical, Ltd. (Mumbai, India). Double-distilled water (D.D water) was used in this study.

2.2. Fabrication of polymer blend electrolyte films

2.2.1. Synthesis of nano-piroviskite La_2CuO_4

In the current investigation, La_2CuO_4 NPs was synthesized based on the sol-gel technique auto combustion method.[27] The appropriate amounts of $La(NO_3)_3.3H_2O$, Cu $(NO_3)_2.3H_2O$ (where the molar ratio of La:Cu is 0.85:0.15) and glycine ($C_2H_5NO_2$) were dissolved in double distilled water, separately. The molar ratio of fuel to oxidant nitrates was 4:1. The individual solutions were then mixed together and the pH value was adjusted to 8.5 by adding NaOH solution. Then, the solution was constantly stirred at 90 ℃ for 2 h to obtain the dark gel. The gel was continuously heated until the combustion process occurred and a loose powder formed. Finally, the slightly dark brown powder was calcinated at 800 ℃ for 4 h.

2.3. Preparation of core shell PANI-La_2CuO_4 NPs

In order to prepare PANI coated nano-La_2CuO_4;[17,28] 2 wt% of La_2CuO_4 NPs, 11.66 g of aniline monomer, and 8.5 mL of 1 M HCl were added into a round-bottomed flask containing 50 mL distilled water and stirred for 1 h (D.D water) and stirred for 1 h. Then, 50 mL of 0.25 M of $(NH_4)_2S_2O8$ (APS) solution in (D.D water) was added slowly with constant stirring. The reaction mixture was constantly stirred for 2 h the in ice bath and allowed for 24 h for complete polymerization of aniline. The precipitated dull green to the black product of (PANI + La_2CuO_4) was gathered, separated and washed with acetone followed by dilute HCl and then with (D.D water). Finally, the solution was filtered and washed with (D.D water) and dried at 60 ℃ in a hot air oven for 1 day to get powder of (PANI + La_2CuO_4), which is stored in desiccators to prepare the blend with PVA.

2.4. Casting of PVA/(PANI+La_2CuO_4)/$LiClO_4$-PC blend SPE films

In the first step, 21 g PVA was dissolved in 300 ml distilled H_2O under a controlled water bath in the temperature range of 80-90 ℃ with constant stirring for 4 h. Then, 20 wt% of PANI was added to 80 wt% of PVA solution with constant stirring for 2 h and sonicated the blend solution for ½ hr. The reaction mixture is poured into cleaned glass petridish and allowed to dry gradually at ambient temperature. In the second step, 20 wt% of core-shell (PANI + La_2CuO_4) was added into the solution of

PVA at 25 ℃ with continuously stirring for 2 h followed by sonicated for ½ hr. The mixture was poured on cleaned and releasing agent coated petridish and let to dry under ambient temperature for 1-3 days. In the third step, 10 wt% of $LiClO_4$ without and with 2, 4, 6 and 8 wt% PC as plasticizers were added separately to the PVA/(PANI + La_2CuO_4) with continuously stirring for 1 h and sonicated for ½ hr. The solution mixture was poured into a mold and left to dry gradually at 25 ℃. Finally, all obtained SPE films were completely dried inside the oven for 4 h at 60 ℃. The thickness of all films was measured where the average thickness is ~0.22 mm.

2.5. Preparation of electrolytes and working electrode

The electrolyte was prepared by dissolving 2 M KOH as an electrolyte in 25 mL of double-distilled water. The prepared films of PVA and its PVA-SPEs have been used directly as the working electrode to check the response of films toward redox reaction and its electrochemical stability. The dry film with a dimension (3cm × 1cm) was connected to an electrochemical cell and immersed in 2 M of electrolyte solution and scanned against Ag/AgCl as reference electrode and platinum wire as a counter electrode.

2.6. Characterization methods

The size and compositional characteristics of the synthesized La_2CuO_4 NPs are studied by Transition Electron Microscope (TEM) with JEOL/JEM 2100, Japan. The structure of PVA-SPEs were obtained at room temperature by X-ray diffraction (XRD) patterns on a D8 Advance-Bruckers AXS diffractometer (Bruker-AXS, USA), with Cu-Kα radiation source (λ = 1.54 Å) operated at 40 kV and 40 mA in the 2θ range 10-80° at the scan speed of 0.05° per second. The morphological behaviors of samples were recorded by scanning electron microscope (SEM), Zeiss-108A, Germany. The physical interaction between components was studied by Fourier transform infrared (FTIR) spectra, JASCO 4100 spectrometer, Japan. All films scanned over the wave number range 4000-500 cm^{-1}. The I-V and ac-electrical parameters of films were measured by LCR-meter Wayane Kerr-6430, the UK at room temperature, where ac-electrical studies in the frequency range 50Hz-5MHz at 1V. Electrochemical cyclic voltammetry (CV) was performed using (CH-Instrument, model 600D series, USA), with potassium hydroxide (2M) as background electrolyte at a potential scan rate of 0.1 $V.s^{-1}$, using Ag/AgCl reference and platinum wire as counter electrodes. The thermal stability of the samples have been studied using thermogravimetric analysis (TGA, TA Instruments Q600, USA) in the temperature range of 30-800 ℃ with a heating rate of 15 ℃/min under a nitrogen gas flow rate of 50 cm^3/min. The UV-visible spectroscopic studies have been established by Schimadzu-1800 spectrophotometer, Japan in the wave-length range of 200-850 nm. Mechanical testing was used to measure the elongation and tensile strength of PVA-SPE films by UTM, ZWICK Z 250, Rowell Material Testing System, Germany.

3. Results and discussion

3.1. Structural and morphological studies

The micro crystalline nature of PVA- SPE films containing 2, 4 and 8 wt% PC were evaluated by XRD. The obtained XRD profiles were displayed in Figure 1. The XRD patterns present the distinctive peaks of the PVA/PANI blend film; an intense peak at 19.8° (hkl = 101) was noticed, which can be attributed to crystalline portions of PVA structure.[29] Besides, peaks at 24.2° and 29.3° are characteristic of PANI,[17,30] which may denote periodically parallel and vertically orientations of PANI chains in its emeraldine salt form.[31,32] The sharp peak at around 18.4° has also resulted from crystalline portions inside the blend structure. XRD patterns for PVA/(PANI + 2 wt%La_2CuO_4 NPs) without and with 10 wt% $LiClO_4$ (Figure 1(b), (c)) displays a small intensity peak at 34.7° ascribed to the presence of La_2CuO_4 NPs,[33] which conformity with the JCPDS card numbers of La_2CuO_4 NPs (JCPDS No.38–0709) that reported earlier.[27]

In addition, a partial decrease of intensity for the main XRD peak at 19.8° as well as the disappearance of peaks at 24.2° and 29.3° have been noticed. It may be due to the physical interaction between Li^+/La_2CuO_4 NPs with functional groups in the blend leading to a reduction in crystalline portions in SPE films. Figure 1(d)-(f) exhibits the effect of introducing PC on crystalline peaks of blend-SPE systems. It was observed that a drastic reduction with broadening in the main peak intensity of PVA in SPEs at 19.8° with increasing in PC contents denote to increase in the amorphous domain in the films. Such trends may be attributed to existence of polarizability of heterogeneous systems such as ions/electrons and dipole for different polar groups leading to increase mutual influence between the components at interfaces causing reduced crystallinity of PVA-SPE films. A similar result was reported else.[34]

Figure 2(a)-(g) shows FTIR spectra of PVA-SPE films. It clearly indicates that the strong and broad peak in the range 3450-

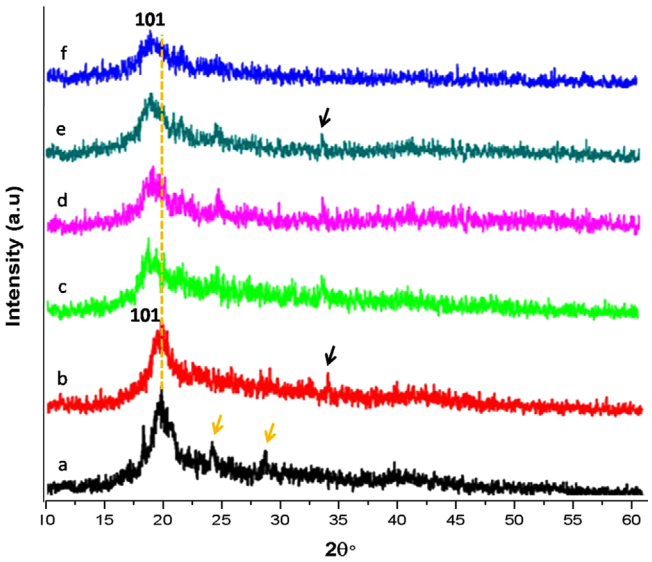

Figure 1. XRD patterns of (a) PPN1, (b) PVA/(PANI+2wt% La_2CuO_4), (c) PVA/(PANI+2 wt% La_2CuO_4)+10 wt% $LiClO_4$, PVA/(PANI+La_2CuO_4)/$LiClO_4$ SPEs with (d) 2, (e) 4, and (f) 8 wt% PC.

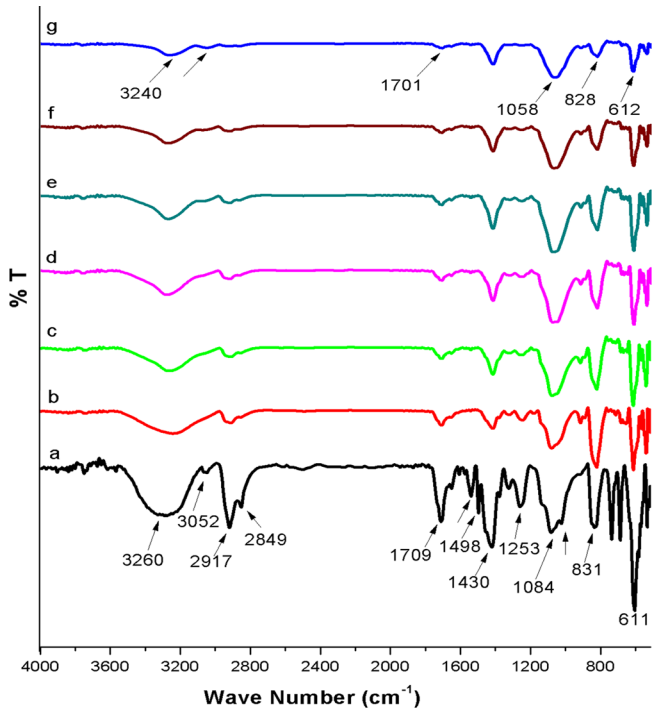

Figure 2. FTIR spectra of (a) PVA/PANI, (b) PVA/(PANI+2 wt% La_2CuO_4), (c) PVA/(PANI+2 wt% La_2CuO_4)+10 wt% $LiClO_4$, PVA/(PANI+La_2CuO_4)/$LiClO_4$ SPEs with (d) 2, (e) 4, (f) 6, and (g) 8 wt% PC.

3200 cm^{-1} with its centering at 3260 cm^{-1} denotes to stretching vibrational of -OH group of PVA interact with a terminal N-H of PANI by H-bonding.[35] This peak intensity was reduced and tends to vanish after an increase in PC content in PVA-SPE, as a result of interaction between NPs/electrolyte and functional groups of PVA/PANI in composites (Figure 2(b)-(g)). The shoulder peak at 3052 cm^{-1} refers to the C=C-H of the aromatic ring which becomes smaller and shifted its position to around 16 cm^{-1} in blend as compared with pure PANI. The symmetric and asymmetric stretching vibration of C-H in PVA skeleton was displayed at 2917 and 2889 cm^{-1} whereas it's bending was noticed at 1430 cm^{-1}. The small vibrational peaks in 1533 and 1498 cm^{-1} for aromatic ring stretching are a typical characteristic of a nitrogen-quinoid structure of PANI in the blend.[36,37] The reduction and disappearance of these peaks in the doped blend denote to the electronic effects by dopants in the PVA-SPEs. The stretching vibration of single bond for residual acetate, O-C-O in PVA was noticed at 1250 cm^{-1}, whilst C-O and C-N of blend show abroad peak with small shoulder and shifted to 1084 cm^{-1} compared with pure PANI.[38]

The peaks at 831 and 730-590 cm^{-1} may be attributed to coupling vibrations of C-H in PVA and aromatic ring.[39] It is noteworthy that the peak at 1140 cm^{-1} observed for pure PANI (Figure 2(a)) shows a very small shoulder in the blend and completely vanishes in the PC loaded SPEs (Figure 2(b)-(g)). It may be due to the protonated amine group ($^{-+}$NH=) oxidizing to imine form (-N=) in composites.[40] The reduced main bands which are shifted to lower wave numbers are found in a doped blend with La_2CuO_4 NPs, $LiClO_4$ and become more significant with increasing PC content. Such trends denote to the interaction between incorporated dopants (fillers/PC) with functional groups

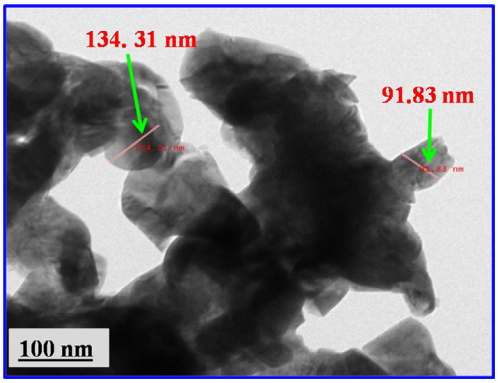

Figure 3. TEM of pristine La_2CuO_4 NPs.

of the blend. Figure 3 exhibits a TEM photo-micrograph for La_2CuO_4 NPs, where the size of La_2CuO_4 NPs lies between 91.8-134.3 nm.

The morphological behaviors of synthesized PANI and PVA/PANI and their PVA-SPE films probed by SEM and obtained images were presented in Figure 4(a)-(f). It can be noticed from Figure 4(a) for pure PANI, the small tubular and porous morphology. The SEM photomicrograph of PVA/PANI (Figure 4(b)) exhibits a semi uniform dispersing of PANI in the PVA matrix. Figure 4(c) shows an SEM photomicrograph for PVA incorporated with core-shell PANI/La_2CuO_4. It can be noticed that the dispersion of coated NPs has small spherical-shaped granules. The roughness of the film was observed after the incorporation of 10 wt% $LiClO_4$ into the blend (Figure 4(d)). However, the roughness of the film was reduced as the concentration of PC increased in the SPE films (Figure 4(e), (f)). It may be due to PC acting as a solvent and assisting in more dissociation of Li salt and preventing them from agglomeration or reforming salt.

3.2. Optical studies

The UV-visible spectra of PVA-SPE films containing varying amounts of PC were displayed in Figure 5(a). From Figure 5(a), the distinctive broad peak at the lower wavelength region for blend at around 245-275 nm is noticed, which refers to n→π^* of PVA.[41] The two peaks at 340-365 nm and 615-640 nm are related to $\pi\rightarrow\pi^*$ transition for the benzenoid ring and n→π^* transition for benzenoid to quinoid of PANI structure, respectively.[42] The broad peak at around 245-275 nm of PVA was affected by the addition of dopants like La_2CuO_4 NPs, $LiClO_4$ and varying amounts of PC. The intensity of absorption peaks increasing with increment additives and it appears partially red shift (284-293 nm), which also corresponds to the absorbance of hybrid La_2CuO_4 NPs for incident light in this region. The small shoulder peak observed for PVA/(PANI+2 wt% La_2CuO_4) at around 320 nm refers to the electronic transition of La_2CuO_4 NPs. For PVA/(PANI+2 wt% La_2CuO_4) SPE films, there is a slight increase of intensity peak at 612-640 nm is ascribed for selective interaction between NPs and quinoid ring in PANI.[43] Furthermore, PVA-SPE containing 10 wt% of $LiClO_4$ showed an increase in absorbance at the peak. Such increment for the intensity of peak may refer to physical interaction between Li^+

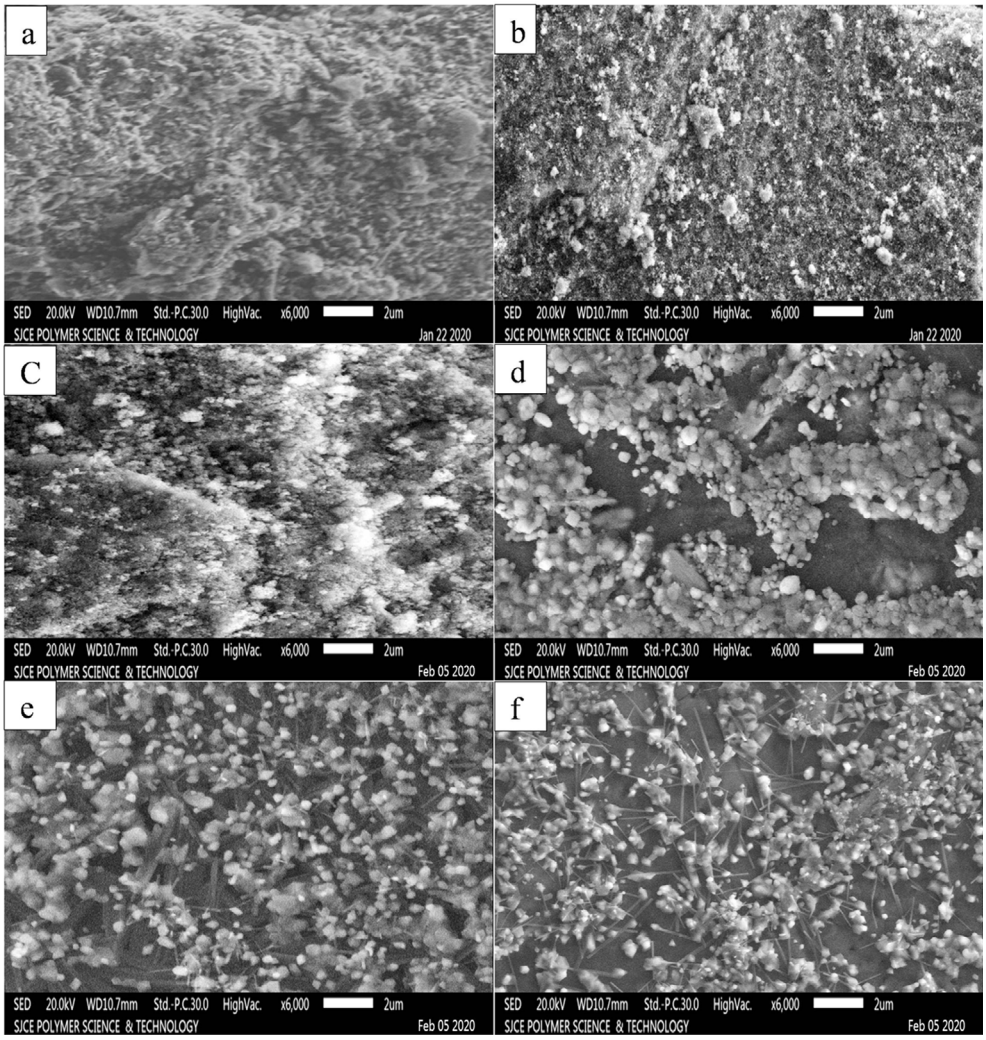

Figure 4. SEM of (a) PANI, (b) PVA/PANI, (c) PVA/(PANI+2 wt% La_2CuO_4), (d) PVA/(PANI+La_2CuO_4)/10 wt% $LiClO_4$, PVA/(PANI+La_2CuO_4)/10 wt% $LiClO_4$ SPEs with (e) 2, and (f) 8 wt% PC.

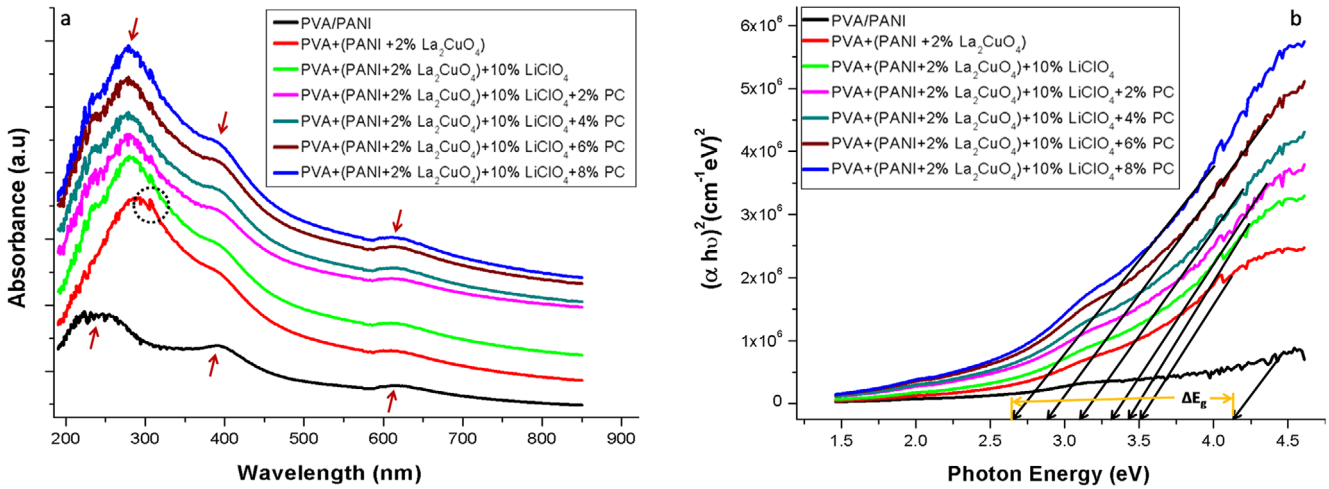

Figure 5. (a) Absorbance *vs.* wavelength and (b) Tauc's plots for PVA-SPEs.

ions with free electrons of nitrogen in PANI and oxygen atoms of PVA chains. Similar trends can be noticed with the addition of PC into NCs which caused to increase in the dissociation of Li salt leading to more interaction with the polymer blend.

The band gap energy, E_g for PVA-SPEs was probed *via* UV-visible spectrum based on Tauc's plots which represent $(\alpha h\upsilon)^2$ versus $h\upsilon$ for direct band gap (Figure 5(b)). The calculated E_g values for all samples were listed in Table 1. The acquired E_g values decreased from 4.2 eV for PVA/PANI to 2.6 eV for PVA-SPE containing 8 wt% PC. Similar kind of behaviors has been

Table 1. Optical parameters of PVA-SPE films

Formulation of SPEs	E_g dir. (eV)	RI (n)
PVA/PANI	4.21	2.11
PVA/(PANI+2% La_2CuO_4)	3.51	2.24
PVA/(PANI+2% La_2CuO_4)+10% $LiClO_4$	3.48	2.25
PVA/(PANI+2% La_2CuO_4)+10% $LiClO_4$+2% PC	3.31	2.28
PVA/(PANI+2% La_2CuO_4)+10% $LiClO_4$+4% PC	3.14	2.32
PVA/(PANI+2% La_2CuO_4)+10% $LiClO_4$+6% PC	2.82	2.64
PVA/(PANI+2% La_2CuO_4)+10% $LiClO_4$+8% PC	2.68	2.45

reported for blend-SPE systems.[44] The decrease in E_g may be due to generating a localized state in band gap where the defects form at the band level in PVA as a result of existing La_2CuO_4 NPs. Moreover, the Refractive index (n) of fabricated PVA-SPEs has been estimated from E_g using Eq. (1):

$$n = K(E_g)^C \quad (1)$$

Where, K and C are constant factors with values (3.3668 and -0.32234), respectively. The calculated results of n for all samples were addressed in Table 1. The n values for all samples are increasing with an increase in dopants contents in PAV-SPE films as compared with PVA/PANI blend may be due to increasing polarization in doped films. The polarization strength increased attributing to the presence of a small ionic radius of positive charge (La^{3+}, Cu^{2+}) in NPs and Li^+ in ionic salt, where it inducing the dipoles of functional groups in the blend polymers (OH in PVA and NH in PANI). Therefore, more interaction with the electromagnetic field of the incident light will occur leading to an increase in the absorption process, thus, n will be increased.[45]

3.3. Electrical and electrochemical behavior

The ac-conductivity (σ_{ac}) dependence on the frequency of PVA/PANI and its PVA-SPEs at room temperature was displayed in Figure 6. It can be noticed from Figure 6 that, the σ_{ac} for all PVA-SPE films tends to increase with increasing frequency, dopants (La_2CuO_4 NPs, $LiClO_4$) and PC contents. The σ_{ac} of blend PVA/PANI exhibits a higher value (6.01×10^{-5} S/cm) as compared with pure PVA (0.82×10^{-5} S/cm) at higher frequencies.[46] It may be due to the presence of conducting PANI in PVA, which improves the σ_{ac} of the blend system. The PANI has conjugated and delocalized the π system in its structure, which is in the resonance state with free-electron of nitrogen atoms caused to flow the current through the system, hence, σ_{ac} increased.

Furthermore, the increase for σ_{ac} in blend SPEs may be due to various factors such as electron tunneling due to the existence of 2 wt% La_2CuO_4 NPs and mobility of dissociated Li ions, where charged carriers move between sites over the potential barrier separating them. Increasing the dosage of PC in SPEs caused the increase in the free volume of segments in polymeric chains, resulting in increased flexibility and mobility of charged carriers through the blend matrix. The increasing PC content in PVA-SPE films to an increase in the dissociation of $LiClO_4$. The estimated σ_{ac} values for all PVA-SPE films were listed in Table 2. The maximum value of σ_{ac} achieved is 4.03×10^{-4} Scm^{-1} for PVA-SPE containing 8 wt% PC.

Figure 7 displays the nonlinear behaviors of log (I) versus ($V^{1/2}$) curves for PVA-SPE films. This deviation or nonlinear in the curves may denote to non-ohmic charge carriers transport process in plasticized blend-SPEs. In insulating PVA, the conduction mechanism through the polymer depends on the injection of electrons from the device to the polymer which undergoes the Schottky mechanism. Whereas, in PVA/PAN blend there is partially modified in the conduction process with existence of

Table 2. Electrical and electrochemical characteristics of PVA-SPE films

Formulations of samples	$\sigma_{ac} \times 10^{-5}$ (S cm^{-1}) ± 1.2%	C_{Spec} (F.g^{-1})
PVA/PANI	6.01	3.25
PVA/(PANI+2% La_2CuO_4)	11.1	4.08
PVA/(PANI+2% La_2CuO_4)+10% $LiClO_4$	14.2	4.49
PVA/(PANI+2% La_2CuO_4)+10% $LiClO_4$+2% PC	17.9	4.68
PVA/(PANI+2% La_2CuO_4)+10% $LiClO_4$+4% PC	25.4	4.91
PVA/(PANI+2% La_2CuO_4)+10% $LiClO_4$+6% PC	34.9	5.12
PVA/(PANI+2% La_2CuO_4)+10% $LiClO_4$+8% PC	40.3	5.45

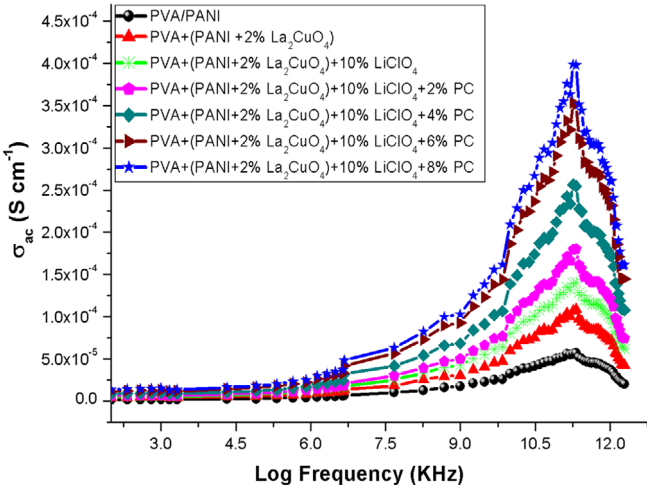

Figure 6. Ac-conductivity *vs.* Log (freq) of PVA-SPEs.

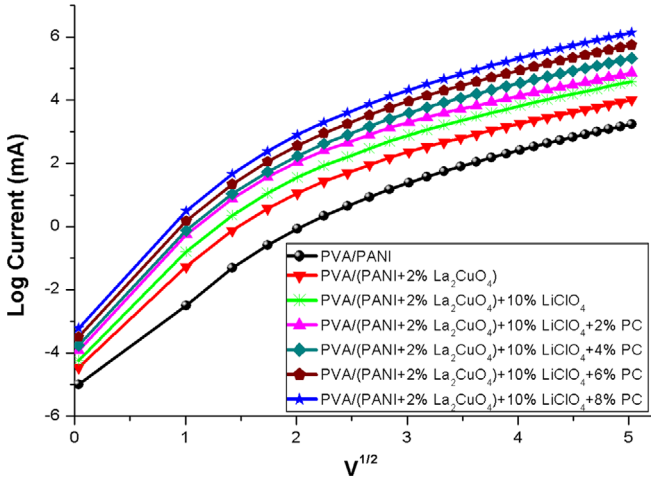

Figure 7. Plots of Logarithmic current *vs.* square root of voltage for PVA-SPEs.

20 wt% PANI where this polymer consists of conjugated double-single bonds, producing an extended π connected network. The diffusion electrons within the π-network are the main source of electric conduction in PVA/PAN.

The fillers are desired for enhancing the conduction process in such kind of blend. The conduction mechanism in SPEs containing NPs and $LiClO_4$ may be due to the electrons diffusion process from NPs accompanied by the ions hopping mechanism in the blend matrix. As the PC content increases in the SPE system, the ions hopping mechanism becomes the most dominant in the electric conduction process.

The cyclic voltammogram was performed to probe the electroactivity of the PVA-SPE films. Figure 8 shows the steady-state voltammograms of PVA-SPEs containing various amounts of PC. In general, all the PVA-SPE films exhibit a good voltammetric response and the oxidation-reduction process as semi-rectangular shapes.

The embedded 2 wt% La_2CuO_4 NPs into PVA/PANI blend showed the semi-rectangular shape and increased current of the redox process with increasing potential voltage as compared with redox process of the undoped PVA/PANI blend. The addition of 10 wt% $LiClO_4$ and different amounts of PC content into PVA/PANI systems increases the current on the CV curves. Therefore, the introduction of La_2CuO_4 NPs, $LiClO_4$ and PC into the blend system leads to promoting movements of charged carriers (electrons/ions) through films, where the dispersion of La_2CuO_4 NPs and Li^+ ions in the blend produces electroactive films. This result indicates that the doped blend could provide an active superficial area or appropriate porous structure which facilitates movements of charged ions, hence increasing current through PVA-SPE films. The CV curves for PVA-SPEs incorporated with PC exhibit higher current as compared with unplasticized films due to the plasticization effect. This interesting result, since it demonstrates that a non-conducting PVA matrix can be successfully integrated into a semi-conductive by PANI coated NPs and electrolyte. The CV curve in Figure 8 denotes that all PVA-SPE films have redox processes between ±4 V and do not decompose or undergo any chemical transformation within the potential region. The higher range of current density and

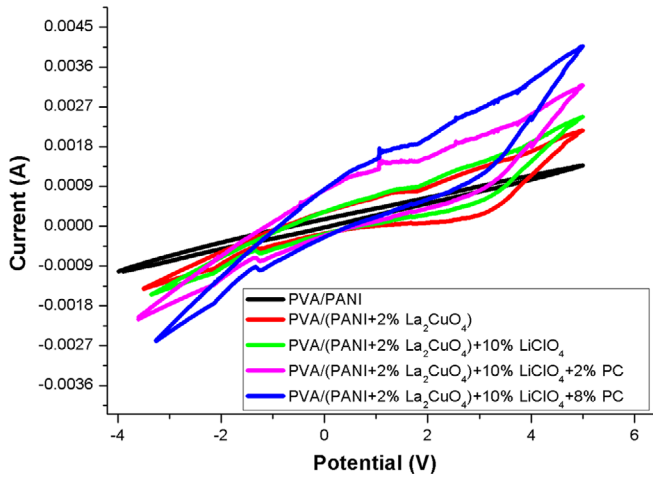

Figure 8. Cyclic voltammograms profiles of PVA-SPE films at scan rate 0.1 $V.s^{-1}$.

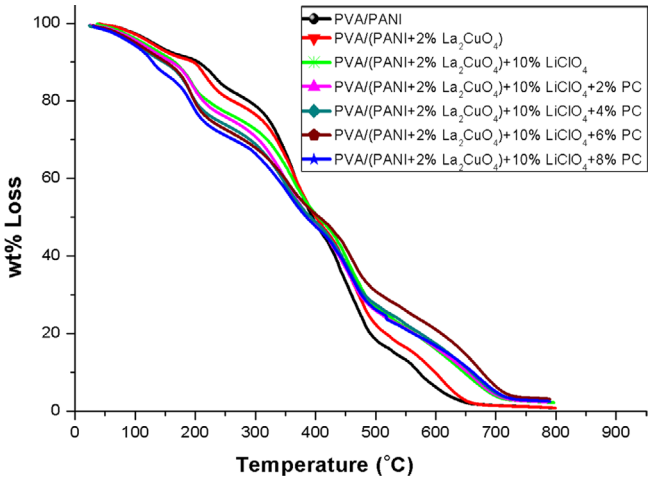

Figure 9. TGA thermograms of PVA-SPE films.

larger semi-rectangular shape of CV curves for PVA-SPE films may denote improvement in the specific capacitance of the system.[47] The calculated C_{spec} for all PVA-SPE films was summarized in Table 2. The obtained results indicate C_{spec} strongly depends on PC content in PVA-SPE films.

3.4. Thermal studies

Thermal degradation patterns for PVA/PANI with its PVA-SPE films were illustrated in Figure 9. The TGA thermo-grams (Figure 9) indicate that the pure PVA/PANI blend undergoes three main steps thermal degradation process. The first thermal decomposition step occurred in the temperature range of 50-150 ℃ with 12% mass loss which ascribes to the release of moisture, low volatile impurities and HCl. The second step occurred in the temperature range of 220-380 ℃ with a corresponding mass loss of around 38%, which is due to the breakdown of side groups and partial decomposition of the blend.[48,49] It is followed by the third step thermal decomposition which occurred in the temperature range of 400-550 ℃ attributing to the degradation of polyene structures in PANI and breakdown of the PVA chain skeleton.[17,50]

With further increase in temperature > 600 ℃, the pyrolysis process will occur and the formation of volatile products. The blend exhibit a similar thermal degradation behavior like pure PVA with a slight reduction in temperature for the decomposition process is observed. The incorporation of 2 wt% La_2CuO_4, 10 wt% $LiClO_4$ and different weight ratios of PC to blends caused a partial reduction in the thermal stability of the system, which may be due to the mutual effects between the components in SPE films. It may be due to an increase in moisture content and the plasticization effect.

3.5. Mechanical studies

Figure 10 shows stress-strain curves of pure PVA, PVA/PANI and PVA-SPE along with different ratios of 2, 4, 6, and 8 wt% of PC. The strain at break of PVA is significantly reduced from ~154.7 to 131.4% because PVA blended with 20 wt% of PANI.

Table 3. Mechanical parameters of PVA/(PANI+2%La_2CuO_4)/$LiClO_4$-PC SPEs

Compositions	Strain at yield (% elongation)	Stress at yield (MPa)	Strain at break (% elongation)	Stress at break (MPa)	Tensile modulus $\times 10^{-1}$ (MPa)	Toughness (Joule)
PVA	72.23	41.02	154.7	48.57	7.747	1.547
PVA/PANI	66.58	33.39	131.4	40.57	6.762	1.318
PVA/(PANI+2%NPs)	55.47	33.55	134.1	42.42	8.463	1.344
PVA/(PANI+2%NPs)/10%$LiClO_4$	76.42	33.30	157.6	39.84	5.837	1.291
PVA/(PANI+2%NPs)/10%$LiClO_4$/2%PC	83.64	28.74	164.8	36.06	5.451	1.278
PVA/(PANI+2%NPs)/10%$LiClO_4$/4%PC	83.40	28.05	165.6	34.96	5.352	1.275
PVA/(PANI+2%NPs)/10%$LiClO_4$/6%PC	78.69	29.20	171.1	32.57	4.578	1.261
PVA/(PANI+2%NPs)/10%$LiClO_4$/8%PC	77.79	27.17	172.1	32.10	4.291	1.241

It may be due to PANI being brittle in nature and unable to form a continuous phase film. Therefore, the addition of a high ratio of PANI contents in the PVA matrix reduced the flexibility of blend films. The reduction in mechanical property by incorporation of PANI in other polymeric matrices has been reported elsewhere.[51,52]

In the meanwhile, the data implies that the embedded 2 wt% La_2CuO_4 NPs into PVA/PANI blend caused an appreciably increment in tensile strength at the break from 40.57 to 42.42 MPa and remarkably enhanced the modulus from 6.76 to 8.46 MPa as compared to un-doped blend film. This outcome proposes that La_2CuO_4 NPs may act as reinforcing filler in the blend and oriented over the direction of stress. Besides, the plots of stress-strain display a partial increment of elongation at break values for PVA/PANI containing La_2CuO_4 NPs. This data denotes that the inclusion NPs inside the blend system could ameliorate interaction between components. The physical interaction would take place between the functional group of the polymeric matrix and NPs resulting in slightly improved elongation at break values with ultimate stress values.[53] The partial increase in the toughness of PVA/PANI doped with 2 wt% of La_2CuO_4 NPs was noticed and it is expected due to an increase in the strength of the film. However, introducing 10 wt% $LiClO_4$ in PVA/(PANI+2 wt% La_2CuO_4) leads to decrease in tensile strength from 42.4 to 39.8 MPa (Figure 10), which may denote the plasticizing effect

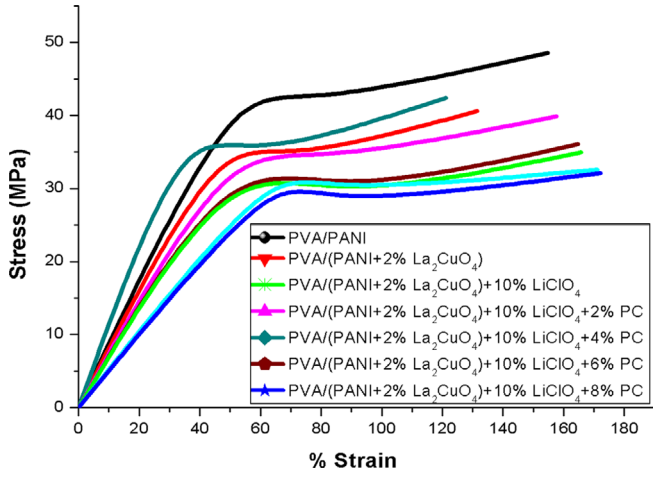

Figure 10. Stress-strain curves of PVA/(PANI+2% La_2CuO_4)/$LiClO_4$-PC SPEs.

of the $LiClO_4$. Possibly, the heterogeneous phase formation of blend/fillers system affects the packing arrangement of the polymeric chains, thereby reducing the tensile strength of blend SPE films which in turn reflects a decrease in the toughness of the film. The data in the table show that reduction in tensile modulus for blend SPE containing 10 wt% $LiClO_4$. A similar result for reducing the modulus for polymeric system doped with 10 wt% $LiClO_4$ was reported elsewhere.[54] The data compiled in Figure 10 and Table 3 reveals an increase in the elongation at break values with increasing PC content in PVA-SPEs, which is due to the increase of flexibility for polymeric segments. At the same time, it indicates the tensile strength and modulus were reduced by a factor ~3-8 MPa, whilst there is no significant changes in the toughness of plasticized PVA-SPE films.

4. Conclusions

The incorporation of plasticizer, PC into SPE blend films had improved the dispersion of NPs and electrolyte. The XRD measurements shown PVA-SPEs have an amorphous domain. The E_g was decreased to 2.68 eV, however, RI increased to 2.45 for PVA-SPE film having 8 wt% PC. The σ_{ac} increases with increasing both frequencies as well the plasticizer contents and the optimum value is found at 4.03×10^{-4} Scm^{-1}. The conducting mechanism of the un-doped blend depends on delocalized π electrons and resonance in PANI structure whilst in PVA-SEPs is the Poole-Frenkel associated with hoping ions mechanism. The specific capacitance of the doped polymer blend is increased to 5.45 F/g as a result of enhance in the mobility of charge carriers. The thermal stability was reduced in SPE films due to increased flexibility by the effect of plasticizer PC. The stress-strain curves of polymer blend electrolyte, PVA/(PANI+2 wt% $LaCuO_4$)/10 wt% $LiClO_4$ containing different ratios of PC have been investigated. In the plasticized PVA-SPEs, the result showed the elongation at break has been increased attributed to increasing flexibility of polymeric segments with the increase in PC content.

References

(1) S. Kim and S. J. Park, *Solid State Ion*, **178**, 973 (2007).
(2) N. Shukla and A. K. Thakur, *Ionics*, **15**, 357 (2009).
(3) X. H. Flora, M. Ulaganathan, K. Kesavan, and S. Rajendran, *Zeits. Phys. Chem.*, **228**, 673 (2014).

(4) N. Rajeswari, S. Selvasekarapandian, M. Prabu, S. Karthikeyan, and C. Sanjeeviraja, *Bull. Mater. Sci.*, **36**, 333 (2013).
(5) A. Arya, S. Sharma, A. L. Sharma, D. Kumar, and M. Sadiq, *Asian J. Eng. Appl. Technol.*, **5**, 4 (2016).
(6) J. Niu, C. Xiaohua, H. Dengwen, C. Liangren, W. Yaping, C. Jianwen, and Z. Yutian, *Chem. Eng. J.*, **424**, 130418 (2021).
(7) C. Jianwen, Z. Yutian, C. Xiaohua, P. Duo, S. Gang, G. Zhanhu, and N. Nithesh, *Adv. Funct. Mater.*, **31**, 2104686 (2021).
(8) J. Chen, F. Wang, G. Zhu, C. Wang, X. Cui, M. Xi, X. Chang, and Y. Zhu, *ACS Appl. Mater. Interfaces*, **13**, 51567 (2021).
(9) S. W. Woo, K. Dokko, H. Nakano, and K. Kanamura, *J. Power Sources*, **190**, 596 (2009).
(10) B. C. Kim, J. S. Kwon, J. M. Ko, J. H. Park, C. O. Too, and G. G. Wallace, *Synth. Met.*, **160**, 94 (2010).
(11) Y. Zhao, H. Wei, M. Arowo, X. Yan, W. Wu, J. Chen, Y. Wang, and Z. Guo, *Phys. Chem. Chem. Phys.*, **17**, 1498 (2015).
(12) A. G. El-Shamy and H. S. Zayied, *Synth. Met.*, **259**, 116218 (2020).
(13) H. M. Gayitri, M. Q. A. Al-Gunaid, F. H. AL-Ostoot, N. Al-Zaqri, A. Boshaala, and A. P. Gnanaprakash, *Polym. Bull.*, DOI: 10.1007/s00289-021-04056-3 (2022).
(14) C. L. Zhu, S. W. Chou, S. F. He, W. N. Liao, and C. C. Chen, *Nanotechnology*, **18**, 275604 (2007).
(15) A. Bekhoukh, M. Mekhloufi, R. Berenguer, A. Benyoucef, and E. Morallon, *Colloid Polym. Sci.*, **294**, 1877 (2016).
(16) L. Zu, X. Cui, Y. Jiang, Z. Hu, H. Lian, Y. Liu, Y. Jin, Y. Li, and X. Wang, *Materials (Basel)*, **8**, 1369 (2015).
(17) B. S. Shashikala, M. Q. A. Al-Gunaid, B. H. Anupama, S. J. Anasuya, and Siddaramaiah, *Polym. Plast. Technol. Mater.*, **60**, 1656 (2021).
(18) B. H. Anupama, M. Q. A. Al-Gunaid, and Siddaramaiah, *Polym. Bull.*, **78**, 3023 (2021).
(19) S. Sugai, Y. Takayanagi, N. Hayamizu, and T. Muroi, *J. Phys. Chem. Solids*, **69**, 3058 (2008).
(20) L. Zhang, Y. Zhang, H. Dai, J. Deng, L. Wei, and H. He, *Catal. Today*, **153**, 143 (2010).
(21) E. R. Macam, B. M. Blackburn, and E. D. Wachsman, *Sens. Actuators B Chem.*, **158**, 304 (2011).
(22) D. K. Pradhan, B. K. Samantaray, R. N. P. Choudhary, and A. K. Thakur, *J. Power Sources*, **139**, 384 (2005).
(23) M. Z. Luisiana, L. Tomas, C. B. Felipe, A. M. Z. Minerva, E. A. S. M. Marisela, D. L. G. Patricia, M. C. Guillermo, R. G. Francisco, N. Guadalupe, and S. V. Saúl, *Mater. Chem. Phys.*, **261**, 124180 (2021).
(24) M. Amid, N. Nabian, and M. Delavar, *Sep. Purif. Technol.*, **251**, 117332 (2020).
(25) M. Q. A. Al-Gunaid, A. M. N. Saeed, and Siddaramaiah, *J. Appl. Polym. Sci.*, **135**, 45852 (2018).
(26) A. M. N. Saeed, A. Hezam, M. Q. A. AL-Gunaid, T. E. Somesh, and Siddaramaiah, *Polym. Plast. Technol. Mater.*, **60**, 132 (2021).
(27) M. Q. A. Al-Gunaid, A. M. N. Saeed, H. M. Gayitri, and Siddaramaiah, *Polym. Plast. Technol. Mater.*, **59**, 469 (2020).
(28) H. Gao, T. Jaing, B. Han, Y. Wang, J. Du, Z. Liu, and J. Zhang, *Polymer*, **45**, 3017 (2004).
(29) T. E. Somesh, M. Q. A. Al-Gunaid, B. S. Madhukar, and Siddaramaiah, *J. Mater. Sci. Mater. Electron.*, **30**, 37 (2019).
(30) B. S. Shashikala, M. Q. A. Al-Gunaid, T. E. Somesh, S. J. Anasuya, and Siddaramaiah, *Polym. Bull.*, DOI: 10.1007/s00289-021-03754-2 (2021).
(31) F. Chen and P. Liu, *Macromole. Res.*, **19**, 883 (2011).
(32) T. M. Wu and Y. W. Lin, *Polymer*, **47**, 3576 (2006).
(33) V. Sami, A. Lambert, and C. Oliver, *APL Mater.*, **9**, 041107 (2021).
(34) S. A. Chandrasekarn, S. Palaniappan, and F. Chandezon, *Mater. Lett.*, **62**, 882 (2008).
(35) A. M. N. Saeed, M. Q. A. AL-Gunaid, and Siddaramaiah, *Polym. Plast. Technol. Mater.*, **57**, 1554 (2018).
(36) S. Honmute, S. V. Ganachari, R. Bhat, H. M. P. Kumar, D. S. Huh, and A. Vankataraman, *Int. J. Sci. Res.*, **1**, 102 (2012).
(37) M. D. Bedre, D. Raghunandan, S. Basavaraj, and A. Venkataraman, *Am. J. Mater. Sci.*, **2**, 39 (2012).
(38) H. M. Gayitri, M. Q. A. AL-Gunaid, Siddaramaiah, and A. P. G. Prakash, *Polym. Bull.*, **77**, 5005 (2020).
(39) J. M. Gohil, A. Bhattacharya, and P. Ray, *J. Polym. Res.*, **13**, 161 (2006).
(40) M. Hasik, A. Drelinkiiewicz, E. Wenda, C. Paluszkiewicz, and S. Quillard, *J. Mol. Struct.*, **596**, 89 (2001).
(41) M. D. Bedre, S. Basavaraja, B. D. Salwe, V. Shivakumar, L. Arunkumar, and A. Venkataraman, *Polym. Compos.*, **30**, 1668 (2009).
(42) P. K. Khanna, N. Singh, S. Charan, and A. K. Visawanath, *Mater. Chem. Phys.*, **92**, 214 (2005).
(43) J. Deng, C. L. He, Y. Peng, J. Wang, X. Long, P. Li, and A. S. Chan, *Synth. Met.*, **139**, 295 (2003).
(44) A. Mostafaei and A. Zolriasatein, *Prog. Nat. Sci. Mater. Int.*, **22**, 273 (2012).
(45) M. Q. A. Al-Gunaid, T. E. Somesh H. M. Gayitri, F. H. Al-Ostoot, and Siddaramaiah, *Polym. Plast. Technol. Mater.*, **59**, 215 (2020).
(46) H. M. Gayitri, M. Q. A. AL-Gunaid, B. S. Madhukar, Siddaramaiah, and A. P. G. Prakash, *Polym. Plast. Technol. Mater.*, **58**, 1110 (2019).
(47) S. El-Sayed, T. Abel-Baset, A. Abou-Elfadl, and A. Hassen, *Physica B*, **464**, 17 (2015).
(48) K. Gurunathan, D. P. Amalnerkar, and D. C. Trivedi, *Mater. Lett.*, **57**, 1642 (2003).
(49) R. Gangopadhyay, D. Amitabha, and G. Ghosh, *Synth. Met.*, **123**, 21 (2001).
(50) H. M. Gayitri, M. Q. A. AL-Gunaid, Siddaramaiah, and A. P. G. Prakash, *Indian J. Eng. Mater. Sci.*, **27**, 320 (2020).
(51) S. Koul, R. Chandra, and S. K. Dhawan, *Polymer*, **41**, 9305 (2000).
(52) B. G. Soares and M. E. Leyva, *Mater. Eng.*, **292**, 354 (2007).
(53) J. K. Rao, A. Raizada, D. Ganguly, M. M. Mankad, S. V. Satyanarayana, and G. M. Madhu, *Polym. Bull.*, **72**, 2033 (2015).
(54) M. Schroers, A. Kokil, and C. Weder, *J. Appl. Polym. Sci.*, **93**, 2883 (2004).